Revista Brasileira de Geografia Física
ISSN:1984-2295
Homepage: https://periodicos.ufpe.br/revistas/rbgfe

Computer modeling of small mobile dams for urban channel application

Jaime Joaquim da Silva Pereira Cabral[1], Yuri Tomaz Neves[2], Arivânia Bandeira Rodrigues[3], José Almir Cirilo[4]

[1] Doutor. em Métodos Computacionais Aplicados à Engenharia pela Wessex Institute of Technology, Professor Associado da Universidade de Pernambuco (UPE) e professor Titular da Universidade Federal de Pernambuco (UFPE), Recife - PE. E-mail: jaime.cabral@ufpe.br (autor correspondente). ORCID: https://orcid.org/0000-0002-1348-8004. [2] Mestre e Doutorando em Engenharia Civil, com ênfase em Recursos Hídricos, pela Universidade Federal de Pernambuco (UFPE), Recife - PE. E-mail: yuutomaz@gmail.com. ORCID: https://orcid.org/0000-0003-0844-2877. [3] Mestra e Doutoranda em Engenharia Civil, com ênfase em Recursos Hídricos, pela Universidade Federal de Pernambuco (UFPE), Recife - PE. E-mail: arivania.rodrigues@ufpe.br. ORCID: https://orcid.org/0000-0003-0452-0006. [4] Doutor. em Engenharia Civil pela Universidade Federal do Rio de Janeiro, Professor Titular da Universidade Federal de Pernambuco (UFPE), Caruaru - PE. E-mail: almir.cirilo@gmail.com. ORCID: https://orcid.org/0000-0002-8672-0898.

Artigo recebido em 30/04/2024 e aceito em 14/10/2024

A B S T R A C T
The increasing need for maintenance and cleaning of urban channels in Recife, along with the complexity and high demand for manual and mechanical services, motivated the development of the "mobile dam," a hydraulic structure that uses a translational wave to clean urban watercourses. This study aims to evaluate the behavior of the wave generated by a small mobile dam, providing a tool that can support efficient management of urban watercourses. The methodology included laboratory experiments with a mobile dam in a concrete channel, monitoring the temporal variation of wave levels. These data were used to calibrate a computational model in the HEC-RAS software, which simulates the wave behavior using shallow water equations. The results showed that the depths ranged from 0.113 m to 0.555 m, with velocities between 1.620 m/s and 1.860 m/s, indicating potential for sediment removal and friction instability in blocks weighing up to 22.5 kg. It is concluded that the mobile dam is effective for cleaning urban channels, although attention is needed for potential erosion risks in channels with non-cohesive materials. The computational modeling proved to be an accurate tool for studying hydrodynamic behavior, providing technical support for urban water management.
Keywords: HEC-RAS; Drag force; Friction instability.

Modelagem computacional de barragens móveis de pequeno porte para aplicação em canais urbanos

R E S U M O
A crescente necessidade de manutenção e limpeza dos canais urbanos de Recife, associada à complexidade e alta demanda de serviços manuais e mecânicos, motivou o desenvolvimento da “barragem móvel”, uma estrutura hidráulica que utiliza uma onda de translação para limpar cursos d’água urbanos. Este estudo visa avaliar o comportamento da onda gerada por uma barragem móvel de pequeno porte, fornecendo uma ferramenta que possa apoiar a gestão eficiente dos cursos d'água urbanos. A metodologia incluiu experimentos laboratoriais com uma barragem móvel em canal de concreto, monitorando a variação temporal dos níveis da onda. Esses dados foram utilizados para calibrar um modelo computacional no software HEC-RAS, que simula o comportamento da onda por meio de equações de águas rasas. Os resultados mostraram que as profundidades variaram entre 0,113 m e 0,555 m, com velocidades entre 1,620 m/s e 1,860 m/s, indicando potencial para remover sedimentos e causar instabilidade por fricção em blocos de até 22,5 kg. Conclui-se que a barragem móvel é eficaz para a limpeza de canais urbanos, embora haja necessidade de atenção a possíveis riscos de erosão em canais com materiais não coesivos. A modelagem computacional demonstrou ser uma ferramenta precisa para o estudo do comportamento hidrodinâmico, oferecendo suporte técnico à gestão de águas urbanas.
Palavras-chave: HEC-RAS; Força de arrasto; Instabilidade relacionada à fricção.

Introduction

Dams are hydraulic structures designed to hold back a water course, contributing significantly to the development of civilization and are one of the most important infrastructures made by man aiming at the more rational use of water resources with different objectives such as energy use, flood control, capture of water for irrigation or water supply, regularization of levels for river navigation, energy generation, waste disposal (Gomes Jr et al, 2024).

For each of the aforementioned objectives, there is a lay-out for the dams, including water intake, spillways and floodgates. Several other devices may come to integrate the system and the general arrangement is a function of a number of aspects, not just hydraulic and hydrological, but also technical, economic and environmental factors. Dam construction has been practiced since the beginning of civilization, and the oldest dam must have been built 6,800 years ago in ancient Egypt (Massad, 2010).

A new type of small dam was developed with the objective of cleaning the sediments accumulated in streams and channels in the plain of Recife, and periodically carry out the maintenance of the urban drainage system.

The device, called “Mobile Dam” was designed by a city engineer, having registered the technological patent. This device applies a methodology for cleaning some city channels that offer certain geometric characteristics for its applicability, and the main one is that the body of water has, at least, lining on the side walls. The equipment consists of a resistant tarpaulin fixed to a metal lattice structure that moves along the stream channel. The operation is based on the closing of a gate, after filling the tarpaulin with subsequent opening, providing a discharge that aims to drag waste downstream, mainly suspended waste, promoting superficial cleaning of the channel (Recife, 2022).

The motivation for the invention arose when observing the difficulty that several municipalities have in maintain major drainage systems in satisfactory cleaning conditions, often performed on an annual basis and manually or mechanically (in cases where there is possibility of access to machinery) with the use of backhoes in small section channels and hydraulic excavators or drag-line in the widest channels.

The mobile dams were initially implemented in Recife, in the Northeast Region of Brazil (State of Pernambuco), which is located at the confluence of several rivers, with low altitude in relation to sea level and high rainfall. Currently, it is the largest urban area in the state of Pernambuco and its metropolitan region is home to a population that exceeds 4 million inhabitants. The demographic density in Recife is around 7,333 inhabitants per km^2, divided into 94 neighborhoods (IBGE, 2022).

Brazilian Venice, as it is recognized, due to the large number of rivers and streams, consisting of 99 canals, approximately 133 km long, 62.4% of which are lined. The microdrainage comprises 1,558 km of galleries and channels, that flow through their territory in different directions (EMLURB, 2017).

The channels accumulate large amount of sediments throughout the year. Thus a periodic cleaning is needed to keep water running in channels ensuring a permanent drainage without the risk of obstructions.

The cleaning of the channels was usually done through excavators that removed the sediment of the channel by placing them in buckets to be transported to the municipal landfill, very far from most of the city's channels.

The usual method implies a great expense and generates numerous inconveniences such as slow traffic resulting from the low velocity of the excavators and the large size of deposits that take more than one lane of the road, in addition to dropping fragments of mud through the streets and cause damage to sidewalks and flowerbeds Therefore, the implemented technique has provided maintenance without many impacts on public places (Cabral & Alencar, 2005).

Given the context that the city is a complex system that consists of many interacting subsystems. And resilience, as a dynamic process, focuses on both the inherent robustness and the adaptive capacity of the city (Ribeiro & Gonçalves, 2019), this technique can be considered as an engineering resilience strategy, highlighting its importance in planning and public policies.

Although the concept of movable dams has its roots in established hydraulic principles, their implementation in urban environments has only recently gained traction, with notable examples in cities such as Recife and other large urban areas.

The channel cleaning procedure using mobile dams in the city of Recife has been carried out by the Urban Cleaning and Maintenance Company (EMLURB). Mobile dams were also used in the cities of Maceió (Alagoas State) and Aracaju (Sergipe State). In Maceió, the Municipal Superintendence of Sustainable Development (SUDES) uses two pieces of equipment: a smaller one, for channels up to six meters wide and one larger, for channels up to 16 meters wide. In Aracaju, the Municipal Company of Urban Services (EMSURB) uses the practice in the channels located in areas difficult to access.

The dynamics of the flow when the tarpaulin is released is reminiscent of a dam breaking. A dam failure problem is a catastrophic event that evolves rapidly, causing large, uncontrollable floods downstream (Gomes Jr et al, 2024). Despite the increase in the ability to design and build safer and more efficient dams in recent decades, more than 200 dams have failed around the world in the 20th century alone (Luino et al, 2014).

The propagation of wave translation after the rupture of a dam has been extensively studied in Brazil, mainly due to some accidents like the rupture of the Camará dam in 2004 in the municipality of Alagoa Nova (Mariano Neto et al., 2017), the Fundão dam in 2015 in the municipality of Mariana (ANA, 2017), and the Córrego do Feijão dam, in 2019 in the municipality of Brumadinho (ANA, 2019; Casagrande et al, 2020).

The one-dimensional flow continuity and momentum equations were developed by Saint-Venant. More recently, the mentioned equations have been used in a more complete way to represent the propagation of the flood wave due to the rupture of dams (USACE, 2014).

Some ways of solving Saint-Venant's equations have been developed by several researchers in an analytical or semi-analytical way adopting several considerations in relation to the opening time and the bottom friction coefficient (Ritter, 1892; Dressler, 1954; Whitham, 1955; Lauber and Hager, 1998; Chanson, 2005).

The first numerical models were based on the 1D Saint Venant equations, also known as 1D shallow water equations (1D-SWEs). These models were widely used in the 80s and 90s to model river floods, with HEC-RAS 1D being the most widespread model (Cea & Costabile, 2022).

One-dimensional models have simpler calculation and implementation procedures and require less computational demand than 2D models; however, when it comes to the propagation of a wave beyond the river channel (unconfined floodplains), 2D models can show better accuracy of flood waves (Palu and Julien, 2020; Paiva et al, 2020).

In the last decades, the tendency is to perform simulations using computational models that have become powerful tools to describe and study processes of runoff in water courses. However, to build a reliable computational model it is necessary to have field data or carry out practical experiments that allow the parameter calibration.

A model that has been widely used to study the hydrodynamic behavior of flows generated by the rupture of dams is the HEC-RAS, developed by the United States Army Corps of Engineers (USACE, 2014).

HEC-RAS offers many tools, such as one-dimensional (1D) constant flow calculation; one-dimensional and two-dimensional (2D) calculation of sediment transport flow; modeling mobile beds and water temperature and quality, presenting results with satisfactory precision and free software availability, in addition to contributing to the management of flooded areas and flood insurance (USACE, 2024a; Oliveira et al, 2022).

In the use of HEC-RAS for dam break analysis, the use of model equations for downstream routing of the dam must combine propagation and reserve in the plain, spatial discretization with controlled interval, control of the Courant criterion and change in the Manning's coefficient (USACE, 2014).

In several countries, HEC-RAS has been applied to study dam rupture. Pilotti et al. (2020) simulated the rupture of the Cancano I dam (Italy), Winarta et al. (2019) simulated the rupture of the Chereh dam (Malaysia), Khosravi et al. (2019) simulated the rupture of the Sefid-Roud dam (Iran).

In Brazil, several studies have been carried out using HEC-RAS to simulate the spread of the flood wave resulting from the rupture of dams. Vieira et al. (2019) analyzed the influence of consideration of the physical mechanisms that cause instability in the human body when defining risk areas. For this purpose, a simulation of the flood wave propagation resulting from the hypothetical rupture of the Santa Helena dam in Bahia state was carried out. Santos et al. (2019) evaluated the behavior of flood wave caused by the hypothetical rupture of the Juturnaíba dam in Rio de Janeiro state. Neves et al. (2021) simulated the hypothetical break of the Jucazinho dam in Pernambuco state. Scenarios were simulated using the breach formation times of 0.1h and 0.5h, seeking to assess the impacts on riverside occupations in two cities.

Almeida et al (2023) evaluated the propagation of uncertainty in the Manning roughness coefficient using a two-dimensional hydrodynamic model in the hypothetical failure of the Três Marias dam, located in the middle stretch of the São Francisco River, Brazil. Pereira et al. (2024) analyzed the hypothetical cascade failure of four dams located in the city of Caruaru - PE.

In this perspective, the present paper aims to evaluate the behavior of the wave generated in a small mobile dam through computational modeling aided by experimental analysis.

Material and methods

The methodology of the present study was divided into three stages: description and functioning of the technique, experimental analysis and computational modeling. In the experimental analysis, a small mobile dam was used to generate translational waves and understand the hydrodynamic characteristics. Furthermore, data were collected to adjust physical and mathematical parameters for computational modeling using HEC-RAS.

Description and Functioning of the Technique

The mobile dam consists of a device for interrupting the flow formed by a waterproof tarpaulin placed at the bottom of the watercourse, juxtaposed to the side walls and tied in two cross sections of the channel at the beginning and end of the tarpaulin sheet. In each sections, a support system, formed by metal trusses supported on the river banks, holds the tarpaulin sheet with steel cables.

During low tide, the ends of the tarpaulin, which are attached to the trusses, are lowered so that it sits at the bottom of the channel, where it remains until the water reaches its maximum level. Then the two extremes of tarpaulin are lifted forming a water bubble that dams all the upstream water. As the water level drops again, the tarpaulin starts to play the role of dam. The system prevents the natural flow of the channel with the volume of water retained upstream the tarpaulin.

At low tide, the downstream level reaches a minimum while on the upstream side the water was stored at high tide level plus the contribution of the flow that arrived in the period. At this point, the tarpaulin is untied and the system releases the accumulated water, dragging the accumulated waste in the channel to a predetermined point where it is collected in concentrated form.

This system can be easily moved along successive segments of the channel as well as to other channels and presents surprising results in both practicality and economy.

The Figure 1 shows examples of mobile dams installed on the channel Derby/Tacaruna in Recife, in the Avenida Airton Teles channel in Aracaju and in the Gulandi channel in Maceió.

Figure 1. Examples of mobile dams: 1 - installed on the Derby/Tacaruna channel in Recife - PE; 2 - installed in the channel Avenida Airton Teles in Aracaju - SE; and 3 - installed on the Gulandi channel in Maceió - AL. Source: (Hidromax Construções, 2003; Rodrigues, 2017; SECOM and Antônio, 2014).

Experimental analysis

The experimental study of the small mobile dam was carried out at the Hydraulics Laboratory of the Center for Technology and Geosciences at the Federal University of Pernambuco. A tarpaulin sheet connected by eyelets to the sides and to two cross sections of a concrete channel was used. In the cross section of the channel, the tarpaulin is raised and the tarpaulin is fixed to a metallic lattice, using a nylon rope (in real case a steel cable is used to tie the tarpaulin to the metal truss).

The metallic lattice holds the tarpaulin that behaves like a dam until the water reaches a planned level. At a certain moment, the mooring is released, almost instantly, and the dam breaks, generating a translation wave.

The adjustment of the model parameters was performed by monitoring the temporal variation of the levels reached by the wave in the experiment. For this purpose, graph papers fixed on one of the side walls of the channel, one lamp and two cameras were used.

The graph papers were fixed to the wall and covered with a transparent plastic sheet (commercially sold as contact paper). The contact paper had the purpose of isolating the graph papers from direct contact with water. The horizontality of the graph papers was carefully checked. The lower region of the graph papers initially had difficulties in fixing the contact paper due to the movement of the water and had to be reinforced. The lamp was installed close to the graph papers in order to facilitate reading the filming. The two cameras recorded videos at 30 frames per second, that is, the videos allowed to extract 30 images every second. The images were used to monitor the levels reached by the wave, to define the breach formation time, which for this experiment was approximately 0.45s.

The release of the tarpaulin for the rupture of the dam, as well as the recordings, was carried out by a team of three people and to synchronize the times, a chronometer was used, viewed by both cameras with partial overlapping of the images at the time of recording. In addition, before breaking the dam, a countdown was carried out, in order to facilitate the work in identifying the image corresponding to the instant when the wave began to propagate.

The experiment was carried out in triplicate and then the average of the values was used to adjust the parameters of the computational model. The average value was used in order to reduce errors inherent to experimental sampling. It is worth mentioning that there is no need to have a large number of events to adjust the hydrodynamic model, as the physical environment is well known and the problem variables are few. In each experiment, five sections 25 cm apart were analyzed. In each section, the levels reached by the wave were obtained every two seconds, varying up to eight seconds.

Figure 2 shows the dimensions of the mobile dam used in the research and the scheme assembled to obtain the temporal variation of the levels reached by the wave.

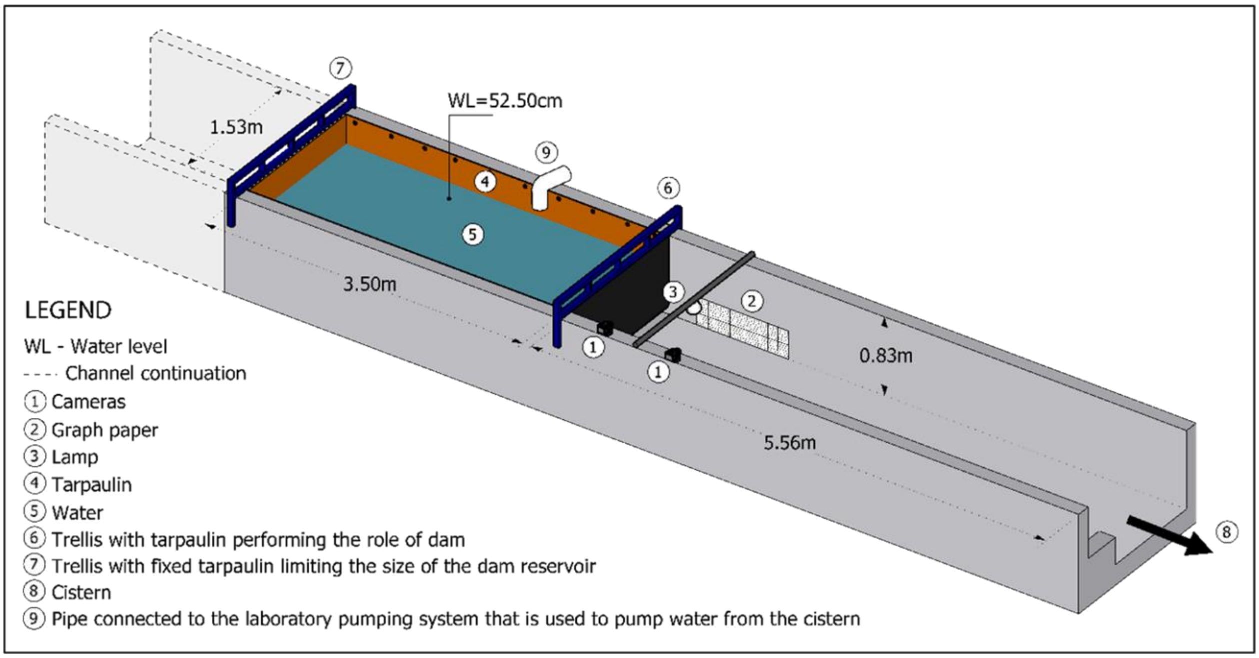

Figure 2. Dimensions of the mobile dam used in the research and the scheme assembled to obtain the temporal variation of the levels reached by the wave.

Computational modeling

HEC-RAS was developed by “Hydrologic Engineering Center” (HEC) of the United States Army Corps of Engineers for “River Analysis System” (RAS). Currently the model performs hydraulic calculations in 1D, 2D and coupled 1D/2D, with steady, quasi-unsteady and unsteady flow regime. The model also makes it possible to analyze water quality, sediment transport, and evaluate the effect of pumping stations and transversal and/or lateral structures to the flow, such as weirs, dams, spillways, gates, levees, bridges and culverts (USACE, 2024a).

Modeling situations such as overtopped and/or breached a levee, in which water can go in many directions, it is recommended to use a 2D modeling. In addition, when modeling events that are very dynamic with respect to time (river systems in which the peak flow comes up very quickly, stays high for a very short time, and then recedes quickly) should generally be used unsteady flow regime (USACE, 2024c). So, the present model was developed using 2D modeling and unsteady flow regime.

In the 2D modeling in unsteady flow regime, the model uses the shallow water equations (also called full Saint-Venant equations in two-dimensions) or the diffusion wave equations. In case of using the diffusion wave equations, the discretization is performed using the finite difference method for time and a hybrid scheme combining finite difference and finite volume methods for the discretization of space. For the cases of using the shallow water equations, the finite volume method is used in the continuity equation and a discretization is applied according to the term of the momentum equation (USACE, 2024b).

The modeling was performed using the shallow water equations. According to USACE (2024a), for the 2D modeling of the dam breaching, it is recommended to use shallow water equations, as they can accurately represent highly dynamic flows. The shallow water equations include two terms that are extremely important in order to accurately model this type of flow, which are: local acceleration (changes in velocity with respect to time) and convective acceleration (changes in velocity with respect to distance).

The shallow water equations in two dimensions are presented below, with Equation 1 being the continuity equation and Equations 2 and 3 being the momentum equations.

$$\frac{\partial H}{\partial t}+\frac{\partial (hu)}{\partial x}+\frac{\partial (hv)}{\partial y}+q=0 \qquad \text{(Equation 1)}$$

$$\frac{\partial u}{\partial t}+u\frac{\partial u}{\partial x}+v\frac{\partial u}{\partial y}=-g\frac{\partial H}{\partial x}+v_t\left(\frac{\partial^2 u}{\partial x^2}+\frac{\partial^2 u}{\partial y^2}\right)-c_f u+fv \qquad \text{(Equation 2)}$$

$$\frac{\partial v}{\partial t}+u\frac{\partial v}{\partial x}+v\frac{\partial v}{\partial y}=-g\frac{\partial H}{\partial y}+v_t\left(\frac{\partial^2 v}{\partial x^2}+\frac{\partial^2 v}{\partial y^2}\right)-c_f v+fu \qquad \text{(Equation 3)}$$

Where: t - time [T]; x and y - cartesian directions [L]; H - water surface elevation (bottom surface elevation plus water depth) [L]; u and v - velocities components in the x and y directions, respectively [LT^{-1}]; h - water depth [L]; q - input/output flow [L^3T^{-1}]; g - gravitational acceleration [LT^{-2}]; f - Coriolis parameter [T^{-1}]; v_t - horizontal eddy viscosity coefficient [L^2T^{-1}]; and c_f - bottom friction coefficient [T^{-1}].

The geometry of the system was developed at HEC-RAS, using the "HEC-RAS Mapper" and the "Geometric Data". Currently, HEC-RAS uses gridded data for 2D modeling. Obtaining the gridded data started with the creation of the geometry of the model in 1D. Then, using the geometry of the model in 1D, a GeoTIFF (*.tif) file was created, which in turn was converted to a Hierarchical Data Format (*.hdf) file, obtaining the geometry in the format that HEC-RAS uses to perform 2D modeling. With the 2D geometry created, the following were added: reservoir and cistern; mobile dam and connection of the channel with the cistern; and 2D mesh along the entire channel. Figure 3 shows the computational model of mobile dam developed at HEC-RAS.

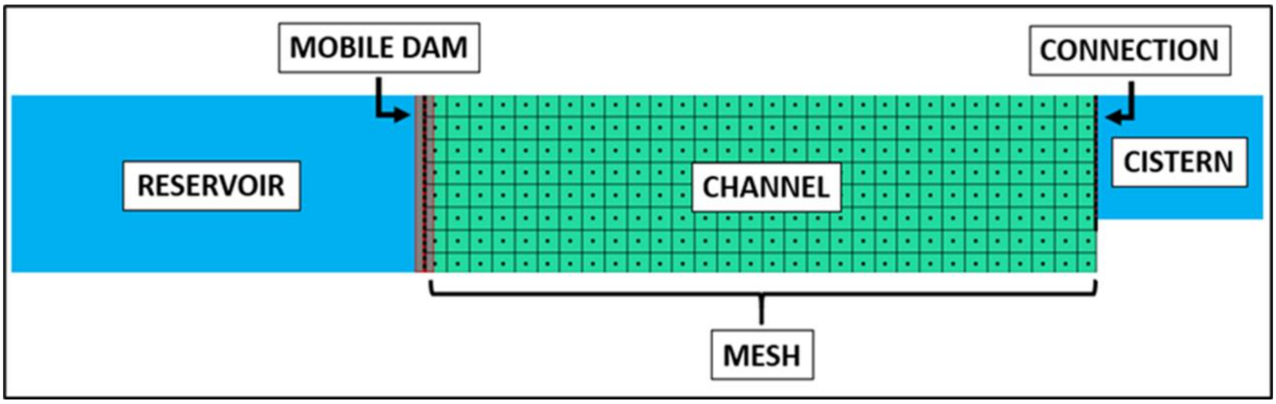

Figure 3. Computational model of mobile dam developed at HEC-RAS.

The mesh was generated in the model itself and can be structured or unstructured. The mesh cells have the following terminologies: cell center, cell faces and cell face points. For each cell, the calculation of the water surface elevation is performed in the center of the cell. Cell faces are lines that boundary the size of the cell. Each cell is limited to have eight faces that control the flow movement from cell to cell. The cell face points, on the other hand, are the ends of the cell faces and are used to hook the 2D flow area to a elements and boundary conditions (USACE, 2024c). Figure 4 presents a scheme with the terminologies used for the model cells.

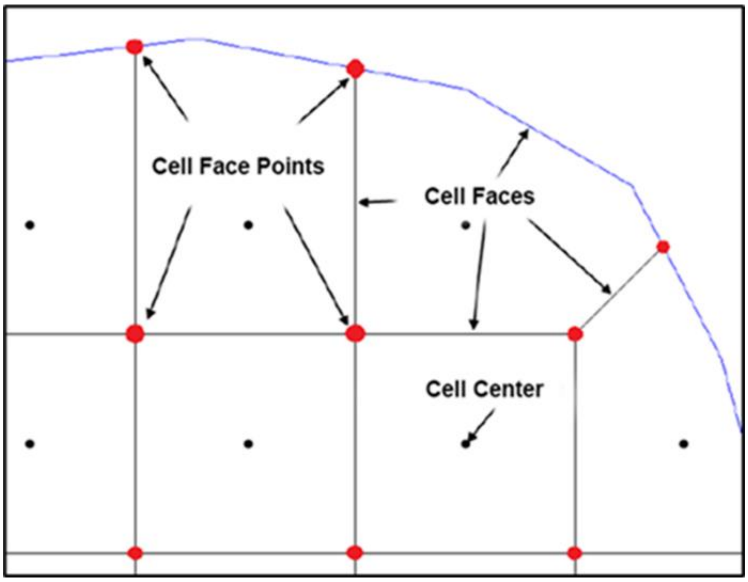

Figure 4. Scheme with the terminologies used for the model cells. Source: USACE (2024c).

The mesh used for spatial representation of the flow in the channel was obtained through the Courant condition, represented by Equation 4.

$$C = \frac{V\Delta T}{\Delta X} \leq 1 \qquad \text{(Equation 4)}$$

Where: C - Courant number (dimensionless); V - Flood wave velocity (wave celerity) (m/s); Δt - Computational time step (s); and Δx - Average cell size (m).

The Courant condition is very important to guarantee the stability and numerical accuracy of the model, especially for situation such dam break modeling. For shallow water equations, a maximum value for the Courant number equal to 3 is allowed. However, if the wave being modeled changes rapidly with respect to time and space, as well as, if the 2D area is started completely dry, the

Courant number close to 1 must be used (USACE, 2024c).

Table 1 presents the values of the Courant number obtained for meshes with different cell sizes tested in the model.

Table 1. Courant number for meshes with different cell sizes tested in the model for Δt=0.10s.

Average cell size (m)	Flood wave velocity (wave celerity) (m/s)	Courant number
0.800	1.387	0.173
0.400	1.563	0.391
0.200	1.797	0.899
0.190	1.844	0.971
0.180	1.853	1.030
0.100	2.379	2.380

According to USACE (2024c), if the water surface slope changes rapidly, then smaller cell sizes need to be used to have enough computation points to describe the changing water surface, as well as compute the force/energy losses that are occurring in that area. For this reason, the computational time step used to calculate the Courant number was 0.1s. For USACE (2024b), extremely small time steps (less than 0.1 seconds) can possibly cause round off errors when storing numbers in the computer, which in turn can lead to numerical errors which can grow over time. The cell sizes were defined as 0.19m x 0.19m which generated a structured mesh with 240cells.

The adjustment of the model parameters was performed manually using the following statistics:

- Nash-Sutcliffe efficiency (NSE): indicates how well the plot of observed versus simulated data fits the 1:1 line. Its value varies from -∞ to 1, where 1 represents the ideal value (Nash and Sutcliffe, 1970). NSE is calculated with Equation 5.

$$NSE = 1 - \left[\frac{\sum_{i=1}^{n} (o_i - s_i)^2}{\sum_{i=1}^{n} \left(o_i - \bar{o} \right)^2} \right] \qquad \text{(Equation 5)}$$

Where: n – is the total number of observations; $\bar{o}$ - mean of n observed water depth values [L]; o_i – is the ith observation for the water depth [L]; and s_i – is the ith simulated value for the water depth [L].

- Percent bias (PBIAS): measures the average tendency of the simulated data to be larger or smaller than their observed counterparts. The ideal value of PBIAS is 0.0. The negative percentage values indicate model overestimation and positive percentage values indicate model underestimation (Gupta et al., 1999). PBIAS is calculated with Equation 6.

$$PBIAS = \left[\frac{\sum_{i=1}^{n} (o_i - s_i) \times (100)}{\sum_{i=1}^{n} (o_i)} \right] \qquad \text{(Equation 6)}$$

Where: n – is the total number of observations; $\bar{o}$ - mean of n observed water depth values [L]; o_i – is the ith observation for the water depth [L]; and s_i – is the ith simulated value for the water depth [L].

- RMSE-observations standard deviation ratio (RSR): incorporates the benefits of error index statistics and includes a scaling/normalization factor, so that the resulting statistic and reported values can apply to various constituents. RSR varies from the optimal value of 0, which indicates zero RMSE or residual variation and therefore perfect model simulation, to a large positive value. The lower RSR, the lower the RMSE, and the better the model simulation performance (Moriasi et al., 2007). RSR is calculated with Equation 7.

$$RSR = \frac{\left[\sqrt{\sum_{i=1}^{n} (o_i - s_i)^2} \right]}{\left[\sqrt{\sum_{i=1}^{n} \left(o_i - \bar{o}\right)^2} \right]} \qquad \text{(Equation 7)}$$

Where: n – is the total number of observations; $\bar{o}$ - mean of n observed water depth values [L]; o_i – is the ith observation for the water depth [L]; and s_i – is the ith simulated value for the water depth [L].

- Determination coefficient (R^2): describes the proportion of the variance in measured data explained by the model. Its value ranges from 0 to 1 and the closer to 1, the better the adjustment (Moriasi et al., 2007). R^2 is calculated with Equation 8.

$$R^2 = \left(\frac{Cov(X_s, X_o)}{\sigma_s \cdot \sigma_o} \right)^2 \qquad \text{(Equation 8)}$$

Where: $Cov(X_S,X_o)$ - covariance between simulated and observed water depth values [L²]; σ_s and σ_o - standard deviation of simulated and observed water depth values [L].

Results and discussion

Initially, the adjustment of the model parameters was carried out using the data of monitoring the temporal variation of the levels reached by the wave in the experiment. After that, the results were explored seeking to understand the behavior of the wave generated in small mobile dams.

In hydrological models, which have a high level of uncertainties and assumed simplifications, the evaluation of these statistics is usually performed through intervals that allow to classify the model's performance. In the adjustment of hydrodynamic models, where the physical environment is well known and the problem variables are few, the aim is to reach the ideal values of these statistics. The parameters used to adjust the computational model were the dam breach weir coefficient and the channel Manning's roughness coefficient. Manning's roughness coefficient refers to the roughness of the bottom and walls of the channel, while the dam breach weir coefficient is a number used to represent the flow behavior during the dam rupture. USACE (2014) presents Table 2 with the guidelines for the selection of the dam breach weir coefficient.

Table 2. Dam breach weir coefficients suggested by US Army Corps of Engineers.

Dam Type	Overflow/Weir Coefficients
Earthen Clay or Clay Core	2.6 - 3.3
Earthen Sand and gravel	2.6 - 3.0
Concrete Arch	3.1 - 3.3
Concrete Gravity	2.6 - 3.0

Source: USACE (2014).

After making the adjustments, the dam breach weir coefficient obtained was 2.36, slightly below the lowest value that is used for earthen clay or clay core, earthen sand and gravel, and concrete gravity dams. This result allows to establish an initial estimate for future studies with modeling of mobile dams at HEC-RAS. Regarding the Manning's roughness coefficient of the channel, the value obtained after the adjustments was 0.012, which corresponds to a value between the minimum and the usual for surfaces with precast concrete covering (Cirilo et al., 2014; Chow, 1959) or smooth surface but with some roughness, small imperfections in alignment and joints (Azevedo Netto and Fernández, 2015; Porto, 2006). It is worth remembering that the channel used in the research is made of concrete. Table 3 shows the statistics obtained after adjusting the model parameters.

Table 3. Statistics obtained after adjusting the model parameters.

Statistics	Analyzed sections (cm)				
	0	25	50	75	100
NSE	0.958	0.924	0.929	0.890	0.627
PBIAS (%)	- 0.161	- 2.773	- 4.563	- 3.292	- 2.766
RSR	0.204	0.275	0.266	0.332	0.610
R²	0.962	0.968	0.955	0.922	0.719

When analyzing the statistics in Table 3, it can be said that the model represented the experiment well up to a distance of 75 cm. For the 100 cm section, it is observed that the results provided by the model are not anymore close to those observed in the experiment.

This was probably due to the influence of the downstream end of the channel. The negative PBIAS values in Table 3 indicate that the data calculated by the model are overestimated.

Behavior of the wave generated in small mobile dams

With the mathematical model adjusted, a study was started to analyze the behavior of the wave, after releasing the volume of water stored in the mobile dam. To situate the reader in relation to the dimensions in the images presented in that item, it is worth remembering that each cell has 0.19 m x 0.19 m. Figure 5 shows the maximum depths and velocities reached by the wave, regardless of time.

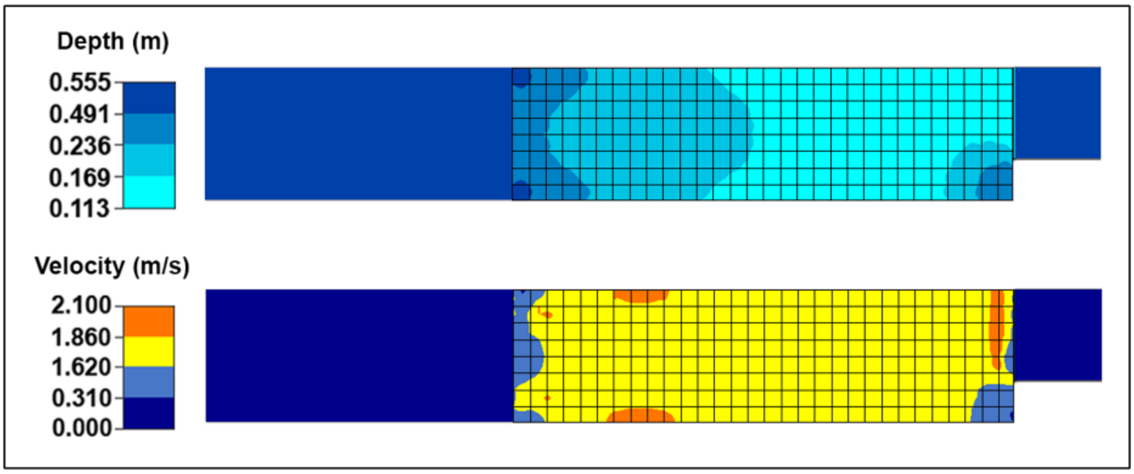

Figure 5. Maximum depths and velocities reached by the wave, regardless of time.

When analyzing Figure 5, it is observed that the maximum depths reached by the wave varied from 0.113 m to 0.555 m, with the values decreasing from upstream to downstream.

Regarding the maximum velocities reached by the wave, it is possible to identify the predominance of values in the range between 1.620 m/s and 1.860 m/s. According to Azevedo Netto and Fernández (2015), these velocities values would pose a risk of erosion in channels with some types of bed materials, such as sandy, gravel and/or other cohesionless materials channels. Therefore, in cases of bed channel with non-cohesive materials, it is necessary to work with an initial water depth lower than that of the present simulation.

It is worth mentioning that depending on the amount of sediment in the section of the channel where the technique is being applied, it may be necessary to carry out several discharges. The channels lined with consistent agglomerated materials, masonry, compact rock and/or concrete, would not present problems of erosion for these velocities values. In addition, these velocities values are well above the average lower limit velocity to avoid the deposition of suspended matter in the water. This shows the strong potential that the wave has in dragging sediments from the channel.

To get an idea of the drag force generated by the wave, two situations were be considered in which rectangular blocks with different characteristics are in the channel during the operation of the mobile dam. Jonkman and Penning-Rowsell (2008) present two equations that relate values of velocities and depths of water to obtain the critical condition from which a block with a rectangular shape is physically impossible to remain in balance. These equations are based on the analysis of two hydrodynamic mechanisms that can cause instability: moment and friction.

Moment instability, also known as toppling, occurs when the moment generated by the drag force exceeds the moment generated by the resultant weight of the block. Friction instability, also known as sliding, occurs when the drag force induced by the horizontal flow is larger than the frictional force between the block and the substrate surface. Figure 6 shows these two instability mechanisms.

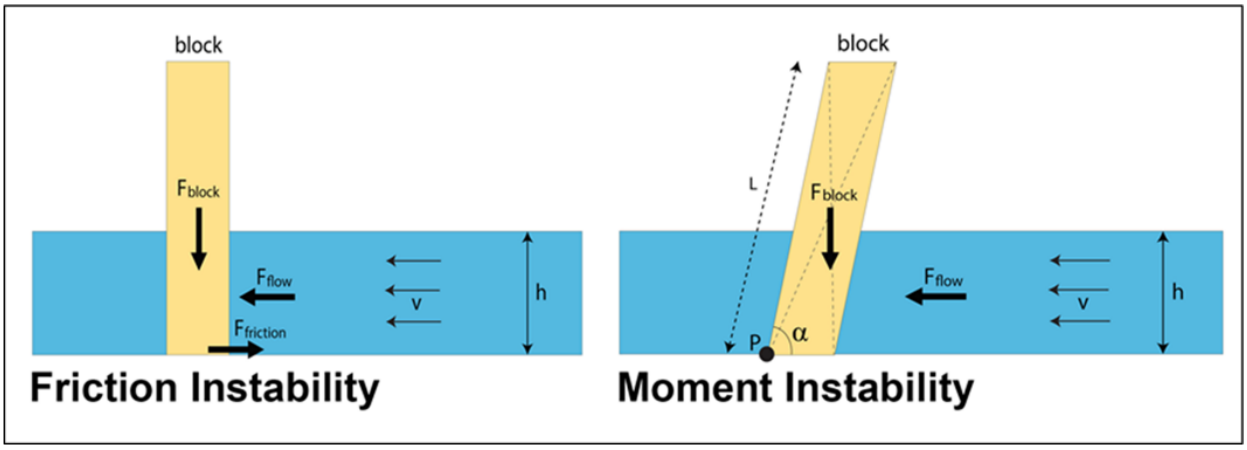

Figure 6. Models of the block for Moment and for Friction Instability. Source: Adapted from Jonkman and Penning-Rowsell (2008).

In the present work, friction instability will be analyzed. This is the last limiting condition. When a block suffers friction instability, it is impossible to remain motionless in place. Any other instability mechanism may happen before friction instability. Jonkman and Penning-Rowsell (2008) present Equation 9 for the calculation of friction instability.

$$hv^2 = \frac{2\mu g}{C_D B\rho} m \qquad \text{(Equation 9)}$$

Where: h - water depth (m); v - flow velocity (m/s); μ - coefficient of static friction (dimensionless); g - acceleration due to gravity (m/s²); m - block mass (kg); C_D - drag coefficient (dimensionless); B - average block width exposed normal to the flow (m); ρ - density of the flowing fluid (kg/m³).

Two artificial blocks of concrete were simulated. Block 1 has dimensions 50 cm x 10 cm x 10 cm and mass of 10 kg. Block 2 has dimensions 50 cm x 15 cm x 15 cm and mass of 22.5 kg. The width of the normal flow face for the two blocks is 50 cm. Endoh and Takahashi (1995) provide values of the coefficient of static friction for different types of surfaces. Based on these values and the characteristics of the small mobile dam channel, a coefficient of static friction of 0.62 was adopted. Jonkman and Penning-Rowsell (2008) adopted the value of 1.1 for the drag coefficient. Considering this value seems to be a reasonable approximation. Acceleration due to gravity was adopted 9.78 m/s² (most accurate number for Recife) and density of the flowing fluid 1000 kg/m³.

According to the formulation proposed by Jonkman and Penning-Rowsell (2008), block 1 and block 2 will slip with values greater than or equal to 0.22 m³/s² and 0.50 m³/s², respectively. Figure 7 shows the results of friction instability for the two blocks, combining the maximum velocities and depths shown in Figure 6.

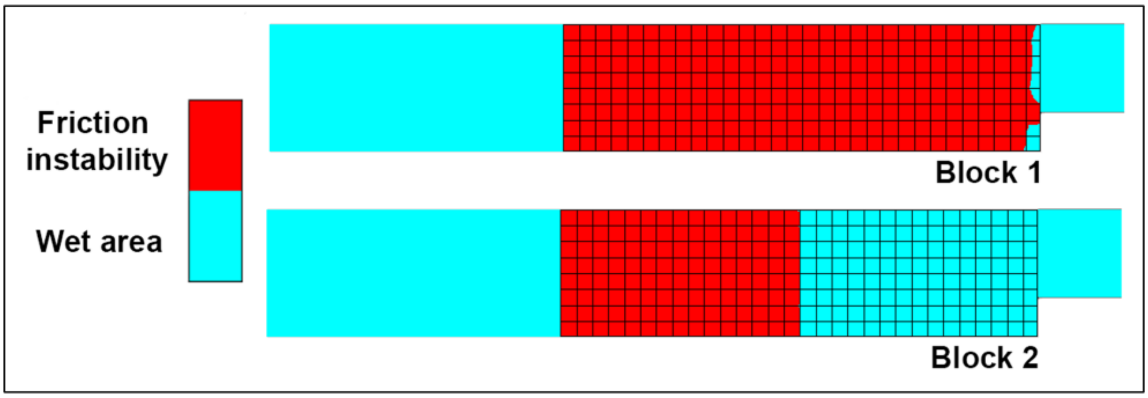

Figure 7. Friction instability for the maximum depths and velocities reached by the wave, regardless of time (mass of block 1 is 10 kg and mass of block 2 is 22.5 kg).

When analyzing Figure 7, it appears that block 1 will be subject to instability in practically the entire channel. For block 2, it is observed that instability will occur uniformly up to a distance of ~2.85 m from the mobile dam. This difference is explained by the fact that the mass of block 1 is less than the block 2. It is noteworthy that this result refers to the combination of maximum velocities and depths that occurred throughout the simulation, regardless of time. This analysis is very important to have an idea if the maximum velocities and depths values were reached at the same time. However, for a more realistic analysis, it is necessary to check the instability in each instant of time. Figure 8 shows the temporal and spatial variation of the wave generated after the dam burst with the friction instability thresholds for the two blocks. When analyzing Figure 8, it appears that the generated wave has the capacity to cause instability in the two blocks. Instability occurs in almost the entire channel for block 1 and only in the initial section for block 2. For block 1: the area of instability tends to increase from 0.4 s to 2.0 s, reaching a distance of ~3.30 m from the mobile dam; at 4.0 s the initial stretch, after the mobile dam, no longer offers a risk of instability and in practically the entire final stretch, which corresponds to a length of ~2.85 m at the end of the channel, the block is subject to slide; after 6.0 s, there is no longer any risk of instability. For block 2: the area of instability tends to increase from 0.4 s to 1.0 s, reaching a distance of ~1.3 m from the mobile dam. After 2.0 s, there is no longer any risk of instability. This result allows us to affirm that up to a distance of ~1.3 m, the wave is capable of causing instability in rectangular objects with a normal face area at a flow of 50 cm x 15 cm and a mass of up to 22.5 kg. Rectangular objects with a normal face area at a flow of 50 cm x 10 cm and that have a mass of up to 10 kg, will be subject to instability in practically the entire channel.

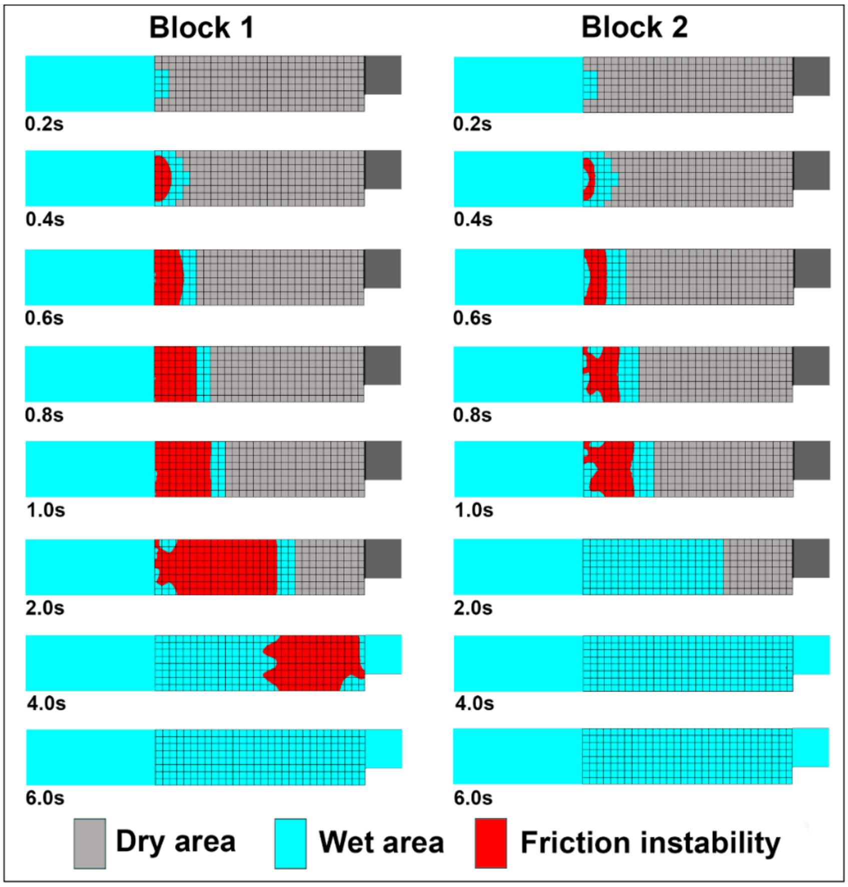

Figure 8. Temporal and spatial variation of the wave generated after the dam breaks with the friction instability thresholds.

Comparing Figures 7 and 8, it is observed that for block 1, the instability analysis combining the maximum depths and velocities, regardless of time, provides results similar to those obtained in the analysis of the temporal and spatial variation of the wave: instability in practically all the channel. For block 2, it is observed that the instability analysis combining the maximum depths and velocities, regardless of time, provides an area greater than ~2.2 times the area obtained in the analysis of the temporal and spatial variation of the wave. The results obtained for block 2 justify the importance of carrying out the instability analysis through the temporal and spatial variation of the wave.

Conclusions

The mathematical model effectively represented the levels reached by the translational wave over time after the release of the movable dam tarpaulin in the laboratory experiment. By fitting the model values, a dam failure coefficient of 2.36 was obtained, which is slightly below the lowest value typically used for clay or clay core dams, earth sand and gravel dams, and concrete gravity dams. This result provides a preliminary estimate for future studies involving modeling of small mobile dams in the HEC-RAS software.

The maximum depths reached by the wave varied from 0.113 m to 0.555 m, with decreasing values from upstream to downstream. The maximum speeds reached by the wave predominantly varied between 1.620 m/s and 1.860 m/s, indicating a strong potential for channel cleaning. However, in channels with a bottom composed of non-cohesive materials, such as sand or gravel, these velocities have a strong potential to cause erosion. Consequently, it may be necessary to modify design conditions and reduce the initial water storage height to achieve lower velocities.

Furthermore, it was found that the drag force generated by the wave is capable of causing instability in a rectangular block with a face area normal to the flow of 50 cm x 10 cm and a mass of up to 10 kg in almost the entire channel. Larger blocks, with a flow-normal face area of 50 cm x 15 cm and a mass of up to 22.5 kg, were susceptible to instability only within approximately 1.3 m of the movable dam.

Urban environment requires the introduction of new practices for planning, management and maintenance of watercourses in cities, especially when it comes from simple, low cost technique with good results. This study provides the first scientific contributions to small mobile dams and aims to contribute to urban water courses management by understanding the functioning of urban mobile dams, thus creating, technical conditions that can support decision making.

Acknowledgments

The authors would like to thank the Coordination for the Improvement of Higher Education Personnel (CAPES) and the Foundation for the Support of Science and Technology of the State of Pernambuco (FACEPE) for encouraging research and granting postgraduate scholarships.

References

Agência Nacional de Águas (Brasil) - ANA. (2017). Relatório de segurança de barragens 2016. Brasília: ANA.

Agência Nacional de Águas (Brasil) - ANA. (2019). Relatório de segurança de barragens 2018. Brasília: ANA.

Almeida, I.M.; Santos, H.A. de Vasconcelos Costa, O.; Graciano, V.B. (2024). Redução da incerteza em áreas de inundação por meio de análises probabilísticas de uso/cobertura do solo em modelos de modelo hidrodinâmico bidimensional de rompimento de barragens. Stoch Environ Res Risk Assess 38 , 1335–1350. https://doi.org/10.1007/s00477-023-02635-6

Azevedo Netto, J. M., & Fernández, M. F. (2015). Manual de hidráulica (9a ed., Volume único). São Paulo: Blucher.

Cabral, J. J. S. P., & Alencar, A. V. (2005). Recife e a convivência com as águas. Gestão do Território e Manejo Integrado das ÁGUAS urbanas, Ministério das Cidades. Brasília, DF.

Casagrande, P.B.; Parisi, M.G.; Moura, A.C.M.; Camargos, L.M.; Zyngier, C.M.; Barbosa, V. S.B.; Magalhães, D.M.; Silva, G.R. (2020). Ruptura de barragem e desastre humano: Córrego do Feijão, Brumadinho, MG. Ciência Computacional e suas Aplicações – ICCSA. ICCSA 2020. Lecture Notes in Computer Science, v. 12255. Springer, Cham. https://doi.org/10.1007/978-3-030-58820-5_61

Cea, L., & Costabile, P. (2022). Flood Risk in Urban Areas: Modelling, Management and Adaptation to Climate Change: A Review. In Hydrology (Vol. 9, Issue 3). MDPI. https://doi.org/10.3390/hydrology9030050

Chanson, H. (2005). Applications of the saint-venant equations and method of characteristics to the dam break wave problem. Brisbane: Department of Civil Engineering at the University of Queensland.

Chow, V. T. (1959). Open-channel hydraulics. New York: Blackburn Press.

Cirilo, J. A., Baptista, M. B., Coelho, M. M. L. P., Mascarenhas, F. C. B., Canali, G. V., Cabral, J. J. S. P., Azevedo, J. R. G., & Montenegro, S. M. G. L. (2014). Hidráulica aplicada (2a ed., Volume único). Porto Alegre: ABRH.

Dressler, R. F. (1954). Comparison of theories and experiments for the hydraulic dam-break wave. International Association of Sciences Hydrology, 3(38), 319–328.

Endoh, K., & Takahashi, S. (1995). Numerically Modelling Personnel Danger on a Promenade Breakwater due to Overtopping Waves. In Proceedings of the XXIVth International conference on Coastal Engineering (ICCE) (p. 1016-1029). Kobe: ASCE.

Gomes Jr, M. N.; Castro, M. de A. R. A.; Silva, P. G. C. da.; Giacomoni, M. H.; Mendiondo, E. M. (2024). Increasing flood awareness through dam-break serious games. International Journal of Disaster Risk Reduction, v.108, 104543. https://doi.org/10.1016/j.ijdrr.2024.104543.

Gupta, H. V., Sorooshian, S., & Yapo, P. O. (1999). Status of automatic calibration for hydrologic models: comparison with multilevel expert calibration. Journal of Hydrologic Engineering, 4(2), 135-143.

Hidromax Construções. (2003). Serviço no canal Derby/Tacaruna em Recife. Recife.

IBGE - Instituto Brasileiro de Geografia e Estatística. (2022). Censo Demográfico. Disponível em: https://www.ibge.gov.br/. Acesso em: 22 jul. 2023.

Jonkman, S. N., & Penning-Rowsell, E. (2008). Human instability in flood flows. Journal of the American Water Resources Association, 44(5), 1208-1218.

Khosravi, K., Rostaminejad, M., Cooper, J. R., Mao, L., & Melesse, A. M. (2019). Dam break analysis and flood inundation mapping: The case study of Sefid-Roud Dam, Iran. In A. M. Melesse, W. Abtew, & G. Senay (Eds.), Extreme hydrology and climate variability: monitoring, modelling, adaptation and mitigation (p. 395-405). Amsterdam, Oxford, Cambridge: Elsevier.

Lauber, G., & Hager, W. H. (1998). Experiments to dambreak wave: horizontal channel. Journal of Hydraulic Research, 36(3), 291-307.

Luino F., Tosatti G., Bonaria V., et al. (2014). Rompimento de barragens no século XX: quase 1000 vítimas evitáveis só na Itália. J. Environ. Ciência e Engenharia, 3, pp. 19 – 31

Mariano Neto, B., Silva, G. R., Cavalcante, M. B., & Silva, M. A. P. (2017). A barragem camará sob os impactos da destruição e reconstrução: um estudo espaço-tempo entre 2004/2014. Revista de Geografia (Recife), 34(2), 56-70.

Massad F (2010) Obras de terra. Oficina de Textos, São Paulo.

Moriasi, D. N., Arnold, J. G., Van Liew, M. W., Bingner, R. L., Harmel, R. D., & Veith, T. L. (2007). Model evaluation guidelines for systematic quantification of accuracy in watershed simulations. American Society of Agricultural and Biological Engineers, 50(3), 885-900.

Nash, J. E., & Sutcliffe, J. V. (1970). River flow forecasting through conceptual models part I - a discussion of principles. Journal of Hydrology, 10(3), 282-290.

Neves, Y. T., Rodrigues, A. B., & Cabral, J. J. S. P. (2021). Modelagem computacional do rompimento hipotético da barragem de Jucazinho no estado de Pernambuco (Brasil). Revista DAE, 69(230), 167-182.

Oliveira, A.M. de.; Conti, J. B.; Santos, R.L.; Oliveira, L.N.A. de.; Brito, C.A.O.; Costa, F.P.; Santana, E.N. (2022). Loss of life estimation and risk level classification due to a dam break. Heliyon, 8, e09257. https://doi.org/10.1016/j.heliyon.2022.e09257

Paiva, C.A. de.; Santiago, A. da. F.; Filho, J. F. do P. (2020). Content analysis of dam break studies for tailings dams with high damage potential in the Quadrilátero Ferrífero, Minas Gerais: technical weaknesses and proposals for improvements. Natural Hazards, 104:1141–1156. https://doi.org/10.1007/s11069-020-04254-8

Palu, M.C.; Julien, P.Y. (2020) Test and improvement of 1D Routing algorithms for dam-break floods. J Hydraul Eng 146(6):1–13. https://doi.org/10.1061/(ASCE)HY.19437900.0001755

Pereira, A. M., Silva, S. R., Pedrosa, H. T. S., Alves, I. S., Oliveira, J. T., Andrade Junior, J. J. A. (2024). Análise da propagação de cheias resultante de rompimentos em cascata hipotéticos de barragens localizadas no município de Caruaru - PE. Revista Brasileira de Geografia Física, 17(1), 529-546.

Pilotti, M., Milanesi, L., Bacchi, V., Tomirotti, M., & Maranzoni, A. (2020). Dam-Break Wave Propagation in Alpine Valley with HEC-RAS 2D: Experimental Cancano Test Case. Journal of Hydraulic Engineering, 146(6), 1-11.

Porto, R. M. (2006). Hidráulica básica (4a ed., Volume único). São Carlos: EESC-USP.

PREFEITURA DO RECIFE/ EMLURB. Plano Consolidado (Resumo Executivo). In: PDDR, ABF Engenharia, Serviços e Comércio Ltda, Recife, 245p., 2017.

Recife (2022). Recife Urban Drainage: between rivers and the sea, the guided and straying waters of Recife, Coleção Recife 500anos, Recife: Cepe.

Ribeiro, P. J. G., & Pena Jardim Gonçalves, L. A. (2019). Urban resilience: A conceptual framework. Sustainable Cities and Society, 50, 101625. https://doi.org/https://doi.org/10.1016/j.scs.2019.101625

Ritter, A. (1892). Die fortpflanzung der wasserwellen. Zeitschrift des Vereines Deutscher Ingenieure, 36(33), 947-954.

Rodrigues, M. (2017). Método de barragem é usado em limpeza do canal da Avenida Airton Teles. Aracaju.

Santos, L. F., Chargel, L. T., & Hora, M. A. G. M. (2019). Simulação do rompimento hipotético da barragem de Juturnaíba, localizada no estado do Rio de Janeiro. Anuário do Instituto de Geociências – UFRJ, 42(3), 299-310.

Secretaria Municipal de Comunicação - SECOM., & Antônio, M. (2014). Prefeito vistoria uso de nova tecnologia para limpeza de canais. Maceió.

United States Army Corps of Engineers - USACE. (2014). Using HEC-RAS for dam break studies. Davis: USACE.

United States Army Corps of Engineers - USACE. (2024a). HEC-RAS river analysis system: user's manual, version 5.0. Davis: USACE.

United States Army Corps of Engineers - USACE. (2024b). HEC-RAS river analysis system: hydraulic reference manual, version 5.0. Davis: USACE.

United States Army Corps of Engineers - USACE. (2024c). HEC-RAS river analysis system: 2D modeling user's manual, version 5.0. Davis: USACE.

Vieira, L. M. S., Fontes, A. S., & Simões, A. L. A. (2019). Analysis of physical mechanisms of human body instability for the definition of hazard zones present in emergency action plans of dams. Case study: Santa Helena Dam, Bahia. Brazilian Journal of Water Resources, 24(43), 1-16.

Whitham, G. B. (1955). The effects of hydraulic resistance in the dam-break problem. Proceedings of the Royal Society A: Mathematical, Physical & Engineering Sciences, 227(1170), 399-407.

Winarta, B., Juwono, P. T., Ali, M. I., & Ramli, N. I. (2019). Dam break studies using hydrologic and hydraulics model for chereh dam, Kuantan, Pahang, Malaysia. In IOP Conference Series: Earth and Environmental Science (p. 1-8). Yogyakarta: IOP Publishing.